Liver and intestinal fatty acid-binding proteins obtain fatty acids from phospholipid membranes by different mechanisms

Alfred E. A. Thumser and Judith Storch[1]

Department of Nutritional Sciences, Cook College, Rutgers University, 96 Lipman Drive, New Brunswick, NJ 08901-8525

Abstract **Intestinal enterocytes contain high concentrations of two cytosolic fatty acid-binding proteins (FABP), liver FABP (L-FABP) and intestinal FABP (I-FABP), which are hypothesized to play a role in cellular fatty acid trafficking. The mechanism(s) by which fatty acids move from membranes to each of these proteins is not known. Here we demonstrate that fluorescent anthroyloxy fatty acid analogues (AOFA) are transferred from phospholipid vesicles to L-FABP versus I-FABP by different mechanisms. For L-FABP a diffusion-mediated transfer process is demonstrated. The AOFA transfer rate from phosphatidylcholine-containing vesicles (POPC) to L-FABP is similar to that observed with another diffusional process, namely inter-membrane AOFA transfer. Furthermore, the AOFA transfer rate was modulated by buffer ionic strength and AOFA solubility, while the transfer rate remained relatively unchanged by the presence of anionic phospholipids in vesicles. In contrast, the data for I-FABP suggest that a transient collisional interaction of I-FABP with the phospholipid membrane occurs during AOFA extraction from the vesicles by the protein. In particular, the presence of the anionic phospholipid cardiolipin in donor vesicles increased the rate of AOFA transfer to I-FABP by 15-fold compared with transfer to POPC vesicles. The effects of ionic strength on transfer suggest that the interaction of I-FABP with cardiolipin-containing vesicles is likely to contain an electrostatic component. Finally, based on the regulation of AOFA transfer to I-FABP compared with transfer from I-FABP, it is hypothesized that apo- and holo-I-FABPs adopt conformations which may differentially promote I-FABP-membrane interactions. In summary, the results suggest that I-FABP, but not L-FABP, can directly extract fatty acids from membranes, supporting the concept that I-FABP may increase the cytosolic flux of fatty acids via inter-membrane transfer.**—Thumser, A. E. A., and J. Storch. **Liver and intestinal fatty acid-binding proteins obtain fatty acids from phospholipid membranes by different mechanisms.** ***J. Lipid Res.*** **2000.** 41: **647–656.**

Supplementary key words fatty acid-binding protein • FABP • liver • intestine

The amphiphilic nature and low solubility of long-chain fatty acids, combined with their large metabolic flux in tissues such as the intestine, liver, heart, muscle, and adipose, suggests a requirement for directed transport processes both between cells and intracellularly (1, 2). Cytosolic transport of long-chain fatty acids is thought to be facilitated by a family of small intracellular proteins (~15 kDa) which display characteristic tissue distributions and are collectively referred to as fatty acid-binding proteins (FABP) (1–6). The exact function(s) of FABPs have yet to be elucidated, but the following roles related to intracellular lipid homeostasis have been proposed: *a*) providing a pool of non-esterified long-chain fatty acids which may be specifically transported and targeted to intracellular sites of metabolism, *b*) modulating lipid metabolic enzyme activity, *c*) protecting against potential detergent-like effects of elevated long-chain fatty acid concentrations, and *d*) modulating lipid-mediated signal transduction and, hence, impacting cell growth and differentiation (1, 2, 5).

The small intestine is the initial site of dietary fatty acid uptake and proximal intestinal enterocytes contain two FABPs, namely liver FABP (L-FABP) and intestinal FABP (I-FABP), at relatively high concentrations (0.1–0.3 mm) (1). Though displaying similar tertiary structures (6, 7), these two FABPs possess overlapping, but different, ligand binding characteristics (2, 6). L-FABP can bind two long-chain fatty acids with differing affinities, as well as other acyl metabolites such as acyl coenzymeA, lysophospholipid, and monoacylglycerol, whereas I-FABP is more restricted in binding only a single long-chain fatty acid (2, 6).

The proposed role of the FABPs as intracellular fatty

Abbreviations: FABP, fatty acid-binding protein; I-FABP, intestinal FABP; L-FABP, liver FABP; SUV, small unilamellar vesicle; AOFA, *n*-(9-anthroyloxy) fatty acids; 12-AO, 12-(9-anthroyloxy)-oleic acid; 12-AS, 12-(9-anthroyloxy)-stearic acid; POPC, 1-palmitoyl-2-oleoyl-phosphatidylcholine; POPG, 1-palmitoyl-2-oleoyl-phosphatidylglycerol; PS, brain phosphatidylserine; PE, phosphatidylethanolamine; NBD-PC; 16:0 12:0-*N*-(7-nitro2,1,3-benzoxadiazol-4-yl)-phosphatidylcholine.

[1] To whom correspondence should be addressed.

acid transporters theoretically requires their direct interaction with ligand donor and acceptor membranes (8, 9). Thus, FABPs may serve not only to deliver long-chain fatty acids to target organelles, but also to remove membrane-bound fatty acids, e.g., exogenously derived fatty acids residing in the inner leaflet of the plasma membrane, or endogenous fatty acids residing in intracellular organellar membranes. Previous studies have suggested that I-FABP delivers fatty acids to acceptor membranes via direct protein–membrane interactions, whereas delivery from L-FABP is modulated solely by the rate of ligand dissociation from the protein (10, 11). The reverse reaction, whereby fatty acids in membranes are transferred to I-FABP and L-FABP, has not been examined at the mechanistic level.

In this study we have investigated the kinetics of fluorescent *n*-(9-anthroyloxy) fatty acid (AOFA) transfer from phospholipid vesicles to L-FABP or I-FABP in order to model the process of fatty acid movement from membranes to FABP. The results demonstrate that AOFA transfer from vesicles to L-FABP is mediated by a diffusional intermediate, whereas a membrane–protein collisional interaction occurs for transfer to I-FABP. This suggests that, for I-FABP in particular, both the extraction and delivery of fatty acids from and/or to membranes occurs via a kinetic mechanism that is subject to regulation by properties of both the membrane and the protein. Thus, I-FABP has the requisite properties to serve as a facilitator and regulator of intracellular fatty acid transport in the enterocyte (8).

MATERIALS AND METHODS

Materials

The anthroyloxy-labeled fatty acids 12-(9-anthroyloxy)-oleic acid (12-AO) and 12-(9-anthroyloxy)-stearic acid (12-AS) were obtained from Molecular Probes (Eugene, OR). Phospholipids were obtained from Avanti Polar Lipids (Birmingham, AL): 1-palmitoyl-2-oleoyl-phosphatidylcholine (POPC), 1-palmitoyl-2-oleoyl-phosphatidylglycerol (POPG), brain phosphatidylserine (PS), bovine heart cardiolipin, egg phosphatidylethanolamine (PE), and 1-palmitoyl-2-(lauryl-*N*-(7-nitro2,1,3-benzoxadiazol-4-yl))-phosphatidylcholine (NBD-PC). Hydroxyalkoxy dextran type VI (Lipidex) was purchased from Sigma. All other chemicals were reagent grade or better.

FABP purification

The pEX-LFABP (liver FABP) and pEX-IFABP (intestinal FABP) expression vectors were generously provided by Dr. Alan Kleinfeld (12) and transformed into BL21(DE3) bacteria (Novagen, Madison, WI) using standard techniques (13). The FABPs were initially purified using a system of gel filtration and ion-exchange chromatography, as previously reported (10, 14), but subsequent purifications utilized hydrophobic interaction chromatography, as follows. Bacterial cells containing the relevant expression plasmid were cultured (37°C) in 2 × YT media (I-FABP) or Terrific Broth (L-FABP) for approximately 4 h before FABP synthesis was induced by the addition of 0.5 mm IPTG and incubation for a further 4 h (13). The cells were collected by centrifugation (4000 *g*, 20 min), re-suspended in cell lysis buffer (50 mm Tris-HCl, 2 mm EDTA, 150 mm KCl, 0.1 mm PMSF, pH 8) and ruptured by sonication. Cellular debris was removed by centrifugation (12 000 *g*, 30 min) and the supernatant was processed in two ammonium sulfate precipitation steps. Initially 2 m $(NH_4)_2SO_4$, 50 mm Tris-HCl, pH 8, was added at a 1:1 ratio (vol:vol) with stirring, followed by centrifugation (12 000 *g*, 30 min). The supernatant fraction was treated with 3 m $(NH_4)_2SO_4$, 50 mm Tris-HCl, pH 8, at a 1:1 ratio and centrifuged (12,000 *g*, 30 min). The latter supernatant fraction (approximately 200 mL in 2 m $(NH_4)_2SO_4$, 50 mm Tris-HCl, pH 8) was loaded onto a Phenyl Sepharose 6FF (high substitution) column (10 cm × 5 cm) (Amersham Pharmacia, Piscataway) equilibrated at room temperature with 2 m $(NH_4)_2SO_4$, 50 mm Tris-HCl, pH 8 (buffer A). The buffer system consisted of two buffers, i.e., buffer A and buffer B (20 mm Tris-HCl, pH 8). The column was initially washed with 300 mL buffer A, then a 500 mL gradient of 100% buffer A–100% buffer B, and finally FABP was eluted by washing the column with approximately 500 mL buffer B. The FABP-containing fractions, as monitored using ^{3}H-labeled oleate, were concentrated using a Miniplate Bioconcentrator system (Millipore Intertech, Bedford, MA), loaded onto a Sephadex G50 gel filtration column (50 cm × 5 cm; 10 mm potassium phosphate, 150 mm KCl, pH 7.4) and the purified FABP was re-concentrated for further use.

The FABPs were delipidated by passage over a Lipidex column, as previously described (15). Protein purity was assessed to be >99% by SDS-PAGE (16) and the protein concentration was determined by the method of Bradford (17), using BSA as standard. Protein concentrations were corrected by factors of 0.6 for L-FABP and 0.95 for I-FABP, respectively (18).

Membrane vesicle preparation

Small unilamellar vesicles (SUV) were prepared with 90 mol% POPC and 10% NBD-PC by sonication and centrifugation in 40 mm Tris-HCl buffer, 150 mm NaCl, 0.1 mm EDTA, pH 7.4 buffer (19, 20). In cases where anionic phospholipids were included in membranes (POPG, PS, cardiolipin) their concentration was 25 mol%, with 65 mol% POPC and 10 mol% NBD-PC. Vesicle phospholipid concentration was determined by quantitating inorganic phosphate (21).

Relative partition coefficients

The partition coefficients (K_p) for AOFA partitioning between FABP and SUVs were determined by measuring AOFA fluorescence at a given molar ratio of FABP:SUV after titration of FABP into a solution containing 25 μM SUVs and 0.5 μm AOFA in 40 mm Tris, 0.1 mm EDTA, 150 mm NaCl, pH 7.4 (22, 23).

$$K_p = ([\text{SUV-bound AOFA}]/[\text{SUV}])/([\text{FABP-bound AOFA}]/[\text{FABP}]).$$

The increase in AOFA fluorescence upon titration of AOFA-containing SUVs with FABP was related to K_p by the following equation:

$$1/\Delta F = (K_p)\,(1/\Delta F_{max})\,([\text{FABP}]/[\text{SUV}]) + 1/\Delta F_{max}$$

where ΔF is the difference between the initial fluorescence of AOFA in SUVs and the AOFA fluorescence at a given FABP:SUV ratio, and ΔF_{max} is the maximum difference in AOFA fluorescence. A plot of $1/\Delta F$ versus $(1/\Delta F_{max})$ ([FABP]/[SUV]) gives a slope of K_p. The partition coefficients were used to establish AOFA transfer assay conditions so as to ensure essentially unidirectional transfer, as detailed below (24).

Kinetics of AOFA transfer from vesicles to FABP

A fluorescence resonance energy transfer assay was used to monitor the rate of AOFA transfer from SUVs to FABP, as previously described for AOFA transfer from FABP to SUVs (10, 14, 25, 26). The fluorescence emission spectrum of AOFA overlaps with the excitation spectrum of NBD and therefore energy trans-

fer occurs when AOFA and NBD are in close proximity, with a resultant quenching of AOFA fluorescence. In the assay system used here, a stock solution of AOFA in ethanol was added to membranes containing 10% NBD-PC (final ethanol concentration <0.5% v/v) such that >98% quenching of AOFA fluorescence was achieved. The AOFA–SUV complex was then mixed with FABP using a Stopped-Flow Spectrofluorimeter DX-17MV (Applied Photophysics Ltd., UK) and transfer of AOFA from donor SUVs to acceptor FABP monitored as the increase in AOFA fluorescence intensity. The excitation wavelengths used were 383 nm and 360 nm for 12-AO and 12-AS, respectively, with emission monitored using a broadband filter (450 ± 35 nm).

The donor membranes typically consisted of 25 μm phospholipid and 0.5 μm 12-AO (L-FABP) or 1 μm 12-AS (I-FABP). The acceptor FABP concentrations were 5 μm L-FABP or 30 μm I-FABP, unless otherwise noted. This disparity in acceptor FABP concentrations was due to differences in AOFA partitioning between membranes and these two FABPs, as sufficient acceptor must be utilized in order to observe unidirectional transfer (10, 25). As shown below, the partitioning data revealed higher relative partitioning for AOFA binding to L-FABP compared to I-FABP, in agreement with previous observations (10). Thus, according to the equilibrium partition data obtained, all kinetic experiments were performed at ⩾1:1 donor:acceptor ratios, taking relative AOFA partitioning into account. In addition, for I-FABP it was necessary to use 1 μm 12-AS as the lower quantum yield for 12-AO bound to I-FABP made detection difficult. Experiments with L-FABP gave qualitatively similar results for 12-AS and 12-AO (see Fig. 1, panel A). Moreover, previous studies of 12-AS and 12-AO transfer from I-FABP to SUVs also demonstrated similar results for these two probes (10, 14). Thus, mechanistic comparisons between the two FABPs are likely to be valid herein. The buffer consisted of 40 mm Tris-HCl, 0.1 mm EDTA, and 150 mm NaCl (pH 7.4), and transfer studies were generally performed at 25°C.

The data were fitted to a mono-exponential equation using the software provided with the stopped-flow spectrofluorimeter. A comparison of data fits to mono-exponential and bi-exponential equations showed that the latter equation did not improve statistical parameters such as χ^2 values, residual-sums-squared, or residual plots (data not shown). Previous studies of inter-membrane AOFA transfer displayed bi-exponential transfer kinetics, indicating that both outer hemi-leaflet AOFA transfer and AOFA flip-flop across the phospholipid bilayer were measured (19). In those studies AOFA were pre-incubated with membrane vesicles for 45 min to allow equilibration of the probe across the phospholipid bilayer (19). Here AOFA ligands were not co-sonicated with phospholipids during SUV preparation in order to minimize the trans-bilayer equilibration of AOFA, and instead the AOFA were pre-incubated with SUVs for only 5 min at room temperature which, as we previously demonstrated, populates primarily the outer hemi-leaflet (19).

Transfer of AOFA between vesicles

Essentially identical conditions were used to measure the rate of AOFA transfer from SUV-to-SUV, as those discussed above for SUV-to-FABP transfer, with the exception that 0.5 mm POPC vesicles were used as the acceptor instead of FABP (27).

Thermodynamics of AOFA transfer from vesicles to FABP

AOFA transfer from SUVs to FABP was measured as a function of temperature and the activation energy (E_A) calculated from the slope of an Arrhenius plot according to the Eyring rate theory (28). The enthalpy of transfer was calculated as $\Delta H^{\ddagger} = E_A - RT$, and the entropy of transfer was calculated as $\Delta S^{\ddagger} = 2.3R \log(NhX/RT)$. R is the molar gas constant, T is the absolute temperature, N is Avogadro's number, h is Planck's constant, $X = k/e^{-\Delta H^{\ddagger}/RT}$ and k is the rate of AOFA transfer from SUVs to FABP determined experimentally at 25°C. Transfer was measured using 25 μm donor SUVs and either 5 μm L-FABP or 30 μm I-FABP as acceptor.

RESULTS

Partitioning of AOFA between FABP and phospholipid membranes.

Determinations of relative partition coefficients for 12-AO between L-FABP and POPC-containing vesicles showed a preferential partitioning to L-FABP by a factor of approximately 18:1 (L-FABP:SUV) (**Table 1**). This value is somewhat lower than that obtained previously for 12-AO partitioning between L-FABP and egg PC vesicles, but similar to the value obtained for 1,6-diphenyl-1,3,5-hexatriene propionic acid partitioning (25, 29). The absolute differences in 12-AO partition coefficients may reflect differences between POPC and egg PC, the latter containing a mixture of acyl chain length phospholipids (as per supplier).

The relative partitioning of 12-AS between I-FABP and POPC vesicles was substantially lower than for 12-AO and L-FABP (Table 1), reflecting the lower equilibrium binding affinity of I-FABP (10). As noted above, the use of 12-AS for studies with I-FABP was necessitated by the low fluorescence quantum yield obtained with 12-AO and I-FABP. In the presence of the anionic phospholipid cardiolipin an increase in the partitioning of 12-AS towards I-FABP was observed (Table 1), which probably reflects charge–charge repulsion between the cardiolipin and the negatively charged AOFA. The observed increase is similar to that obtained for the partitioning of 1,6-diphenyl-1,3,5-hexatriene propionic acid between SUVs and L-FABP, or heart FABP when the anionic phospholipid PS was included with PC in vesicles (29).

All further studies were performed under conditions where the acceptor to donor ratios (FABP:SUV) were above the determined equilibrium partition coefficients (Table 1) in order to ensure uniformly unidirectional transfer in kinetic experiments (10, 25). As described previously for experiments that examined AOFA transfer from FABP to SUVs (10), this means that a greater ratio of SUV:L-FABP as compared with SUV:I-FABP was used when measuring AOFA transfer from SUVs to FABP.

TABLE 1. Coefficients for the partitioning of AOFA between L-FABP or I-FABP and phospholipid membranes

Ligand	SUV (donor)	FABP (acceptor)	Partition Coefficient (FABP:SUV, mol:mol)
12-AO (0.5 μm)	POPC	L-FABP	18.5 ± 3.3
12-AS (1 μm)	POPC	I-FABP	0.8 ± 0.3
12-AS (1 μm)	25% cardiolipin	I-FABP	2.2 ± 0.3

Results are the average of three separate experiments ± standard deviation. The coefficients for AOFA partitioning (K_p) between FABP and SUVs were determined by measuring AOFA fluorescence at a given molar ratio of FABP:SUVs after titration with FABP (22, 23).

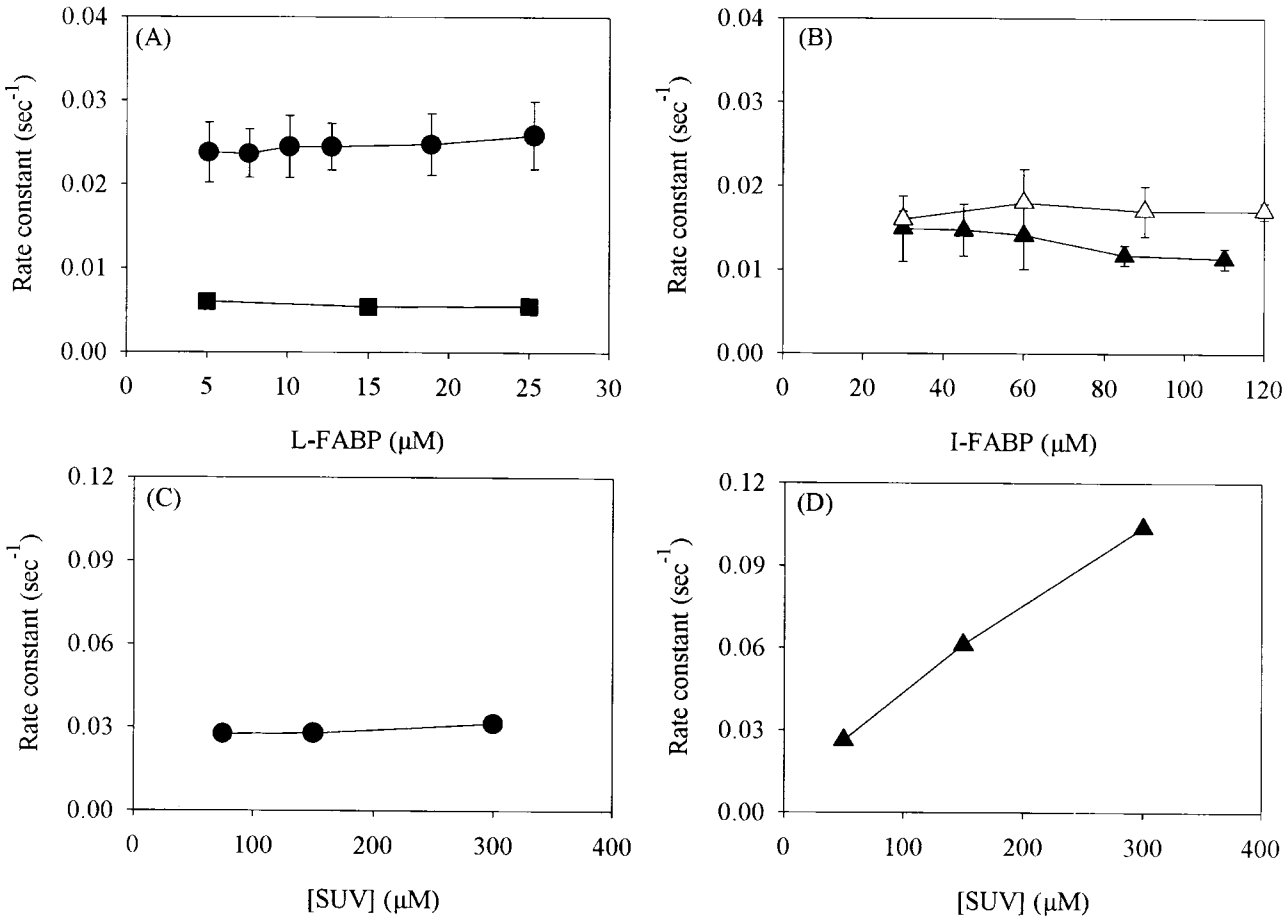

Fig. 1. Effect of acceptor concentration on the rate of AOFA transfer. The acceptors in (A) and (B) are L-FABP and I-FABP, respectively, with membrane vesicles acting as AOFA donor. In (C) and (D), L-FABP and I-FABP are the AOFA donors, respectively, with membrane vesicles as acceptor. (A) Transfer of 0.5 μm 12-AO (●) or 1 μm 12-AS (■) from 25 μm 90% POPC/10% NBD-PC vesicles. (B) Transfer of 1.0 μm 12-AS from 25 μm 90% POPC/10% NBD-PC (▲) or 25 μm 80% POPC/10% egg PE/10%NBD-PC (Δ) vesicles. AOFA transfer from FABP to 90% POPC/10% NBD-PC vesicles was determined with (C) 5 μm L-FABP/0.5 μm 12-AO (●) and (D) 30 μm I-FABP/1.0 μm 12-AS (▲). Transfer was measured at 25°C and rate constants (k) were determined by fitting the data to a mono-exponential equation. Data shown for at least three different experiments ± standard deviation (panels A and B). Single control experiments are shown in panels C and D.

AOFA transfer from zwitterionic membranes to FABP

Effect of acceptor FABP concentration. The AOFA transfer rate from POPC-containing donor vesicles to L-FABP was found to be independent of acceptor L-FABP concentration, suggesting that AOFA transfer is diffusion-mediated (**Fig. 1, panel A**). Also, the 12-AO transfer rate is similar to that obtained for diffusion-mediated inter-membrane transfer utilizing POPC vesicles (**Fig. 2, panel A**) (27). Although somewhat slower than the rate of 12-AO dissociation from egg PC SUVs (19), the latter difference in transfer rate can probably be explained by differences in the phospholipid used (POPC used here vs. egg PC (19)) and we deduce that we are measuring 12-AO dissociation from SUVs. The slower transfer rate observed for L-FABP with 12-AS relative to 12-AO (Fig. 1, panel A) mimics that observed for AOFA transfer between membranes and presumably reflects the difference in aqueous-phase solubility of these two ligands (19, 27). For I-FABP the rate of 12-AS transfer from donor SUVs is also independent of acceptor protein levels. Notably, however, it is 2- to 3-fold higher than the rate obtained for 12-AS transfer from SUVs to L-FABP (Fig. 1, panels A and B).

To directly compare the rate of AOFA transfer from membranes to FABP with that from FABP to membranes, i.e., in opposite directions, transfer from 5 μm L-FABP (0.5 μm 12-AO) or 30 μm I-FABP (1.0 μm 12-AS) was measured as a function of increasing SUV concentration (Fig. 1, panels C and D). The rate of AOFA transfer from L-FABP to SUVs was independent of phospholipid concentration, whereas the transfer rate from I-FABP increased proportionally with phospholipid concentration (Fig. 1, panels C and D), confirming previous results (10).

Effect of ionic strength. The aqueous solubility of ionic amphiphiles is proportional to the salt concentration, and decreases (a salting-out effect) with an increase in the ionic strength of the bulk solvent (30, 31). The rate of AOFA transfer through the aqueous phase, as facilitated by an aqueous diffusion-mediated mechanism, would therefore be inversely related to the salt concentration. In the case of AOFA transfer to L-FABP, a logarithmic decrease in

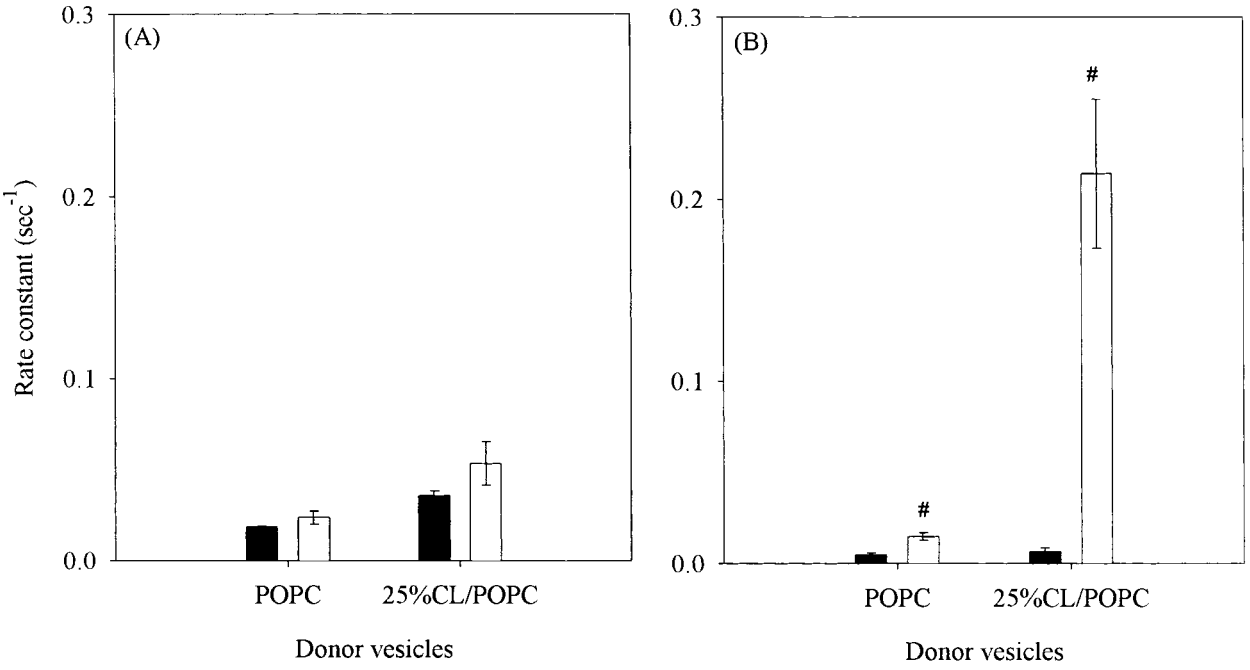

Fig. 2. Comparison of SUV-to-SUV and SUV-to-FABP transfer rates. Transfer of 1 μm AOFA from 25 μm donor vesicles, which contained either 90% POPC/10% NBD-PC or 25% cardiolipin/65% POPC/10% NBD-PC, to 100% POPC acceptor vesicles (solid bars) or acceptor FABP (open bars) was measured. Donor vesicles contained (A) 0.5 μm 12-AO and the acceptor was either 0.5 mm POPC vesicles or 5 μm L-FABP, and in (B) transfer of 1 μm 12-AS to acceptor vesicles or 30 μm I-FABP was measured. Data shown for at least three different experiments ± standard deviation. $^{\#}P < 0.01$ in a comparison of SUV-to-SUV and SUV-to-FABP transfer rates, using the same vesicles as AOFA donor.

the transfer rate is indeed observed (**Fig. 3**), in agreement with previous findings for AOFA transfer from L-FABP to SUVs (10, 32), and supportive of the hypothesis that transfer takes place through an aqueous-phase intermediate.

For 12-AS transfer from SUVs to I-FABP, an increase in AOFA transfer rate is observed with increasing salt concentration (Fig. 3), indicating that a different mechanism of AOFA transfer may occur with I-FABP as acceptor. A similar salt-dependent increase in AOFA transfer rate from heart FABP to SUVs was suggested to indicate collisional interactions between heart FABP and SUVs during AOFA transfer (14, 26, 33). Alternatively, it is possible that the increased transfer rate may be secondary to an alteration in phospholipid bilayer structure at higher salt concentrations (19), and/or to a subtle change in I-FABP structure, as was demonstrated with heart FABP (14). It is worth noting that a change in AOFA transfer rate that occurs as a consequence of altered acceptor I-FABP conformation would support the hypothesis that transfer occurs during membrane–protein interactions, as acceptor properties do not influence diffusion-mediated transfer processes. In any case, the fact that the AOFA transfer rate varies as a function of ionic strength in the opposite direction from that observed with processes dependent on ligand solubility argues against an aqueous-phase intermediate in AOFA transfer from zwitterionic SUVs to I-FABP.

Effect of temperature. The transfer of AOFA from POPC vesicles to both L-FABP and I-FABP was examined at different temperatures from 4°C to 45°C in order to determine the thermodynamic parameters for AOFA transfer. The transfer rate increased with temperature (data not shown) and analysis of the rate constant for AOFA transfer from SUVs to L-FABP or I-FABP demonstrated that the major thermodynamic contribution to $\Delta G^{\ddagger}$ was an enthalpic component (**Table 2**). The decrease in the entropic component was larger for AOFA transfer to L-FABP than I-FABP. Because a decrease in entropy ($\Delta S^{\ddagger}$) is typically interpreted to reflect the ordering of water molecules

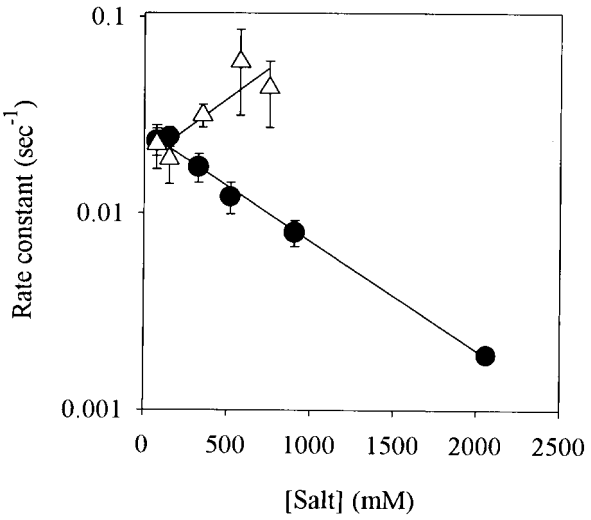

Fig. 3. Ionic strength effect on AOFA transfer rate from donor membrane vesicles to acceptor FABP. Transfer of 0.5 μm 12-AO from 25 μm 90%POPC/10%NBD-PC vesicles to 5 μm L-FABP (●) or 1.0 μm 12-AS from 25 μm 90% POPC/10% NBD-PC vesicles to 30 μm I-FABP (△) was measured as a function of NaCl concentration. Data shown for at least three different experiments ± standard deviation.

TABLE 2. Thermodynamic parameters for AOFA transfer from phospholipid vesicles to L-FABP or I-FABP

Ligand	L-FABP 12-AO (0.5 μm)	I-FABP 12-AS (1 μm)	I-FABP 12-AS (1 μm)
SUV	90% POPC/10% NBD-PC	90% POPC/ 10% NBD-PC	25% cardiolipin/65% POPC/10% egg PE/10% NBD PC
E_a (kcal/mol)	13.4 ± 0.1	16.7 ± 1.5[a]	20.7 ± 0.4[a,b]
$\Delta G^{\ddagger}$ (kcal/mol)	19.9 ± 0.1	19.8 ± 0.1	17.8 ± 0.1[a,b]
$\Delta H^{\ddagger}$ (kcal/mol)	13.1 ± 0.1	16.5 ± 1.5[a]	20.1 + 0.4[a,b]
$T\Delta S^{\ddagger}$ (kcal/mol)	−6.8 ± 0.2	−3.3 ± 1.4[a]	2.4 ± 0.4[a,b]

Results are the average of three separate experiments ± standard deviation. Transfer was measured using 25 μm donor SUVs and either 5 μm L-FABP or 30 μm I-FABP as acceptor.

[a] Indicates $P < 0.05$ when compared to L-FABP, and [b] $P < 0.05$ for transfer from I-FABP comparing POPC- and cardiolipin-containing vesicles.

brought about by aqueous-phase hydrophobic moieties, these results provide further support for a diffusional intermediate in AOFA transfer to L-FABP. The higher enthalpic contribution for AOFA transfer to I-FABP suggests that conformational changes in I-FABP and/or vesicle structure may take place during AOFA transfer, possibly in part as a result of protein–membrane interactions.

AOFA transfer from anionic membrane vesicles to L-FABP and I-FABP

Effect of vesicle charge. Contrasting results were obtained for L-FABP and I-FABP when AOFA transfer from vesicles containing 25% anionic phospholipids was monitored (**Fig. 4**). For transfer to L-FABP, no change was observed with vesicles containing only POPC or POPC with PS or POPG, and a small increase (approximately 2-fold) in transfer rate was observed with cardiolipin-containing vesicles (Fig. 4). The latter increase in the AOFA transfer rate observed with cardiolipin-containing SUVs (Fig. 4) may be explained by electrostatic charge repulsion between the anionic AOFA and the cardiolipin headgroup in these vesicles, as clearly demonstrated in studies of intermembrane AOFA transfer (Fig. 2, panel A) (27).

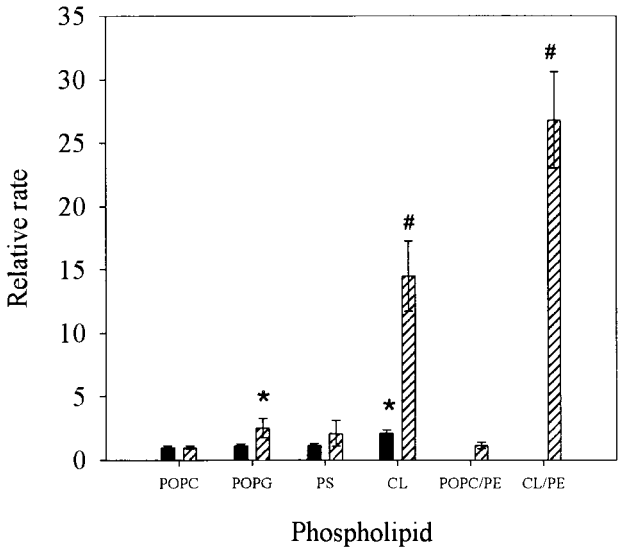

Fig. 4. Effect of donor membrane composition on AOFA transfer rate from donor membrane vesicles to FABP. Transfer from 25 μm vesicles consisting of 25% anionic phospholipid in 65% POPC/10% NBD-PC and 0.5 μm 12-AO to 5 μm L-FABP (solid bars) or 1.0 μm 12-AS to 30 μm I-FABP (hatched bars) was measured at 25°C in 150 mm NaCl buffer. The results are expressed relative to the rate constant obtained for transfer from 90% POPC/10% NBD-PC vesicles. Data shown for at least three different experiments ± standard deviation. * $P < 0.05$ and # $P < 0.01$ compared to data for 90% POPC/10% NBD-PC vesicles. No data are available for L-FABP and vesicles containing egg PE.

In contrast to L-FABP, AOFA transfer to I-FABP increased 2- to 3-fold from PS- and POPG-containing SUVs, and approximately 15-fold from vesicles containing 25% cardiolipin, relative to POPC SUVs (Fig. 4). While POPG, PS and cardiolipin are all negatively charged, at physiological pH the net charge on cardiolipin is −2 as compared to −1 for POPG and PS. Thus, the effects of the anionic phospholipids are apparently not directly proportional to the net charge, suggesting that the markedly increased AOFA transfer rate observed with cardiolipin vesicles and I-FABP may be due to alterations in phospholipid and/or vesicle structure, in addition to charge–charge interactions between cardiolipin and I-FABP. Further evidence for a phospholipid and/or vesicle structure effect on the transitional interaction between I-FABP and membranes during the transfer process is that an additional increase in AOFA transfer rate is observed with vesicles containing 25% cardiolipin plus 10% egg PE, in which net SUV charge is unchanged (Fig. 4). Presumably, this additional increase in transfer rate is due to the well-known effects of PE on bilayer lipid order (34). Regulation of AOFA transfer by anionic vesicles must, therefore, reasonably require a physical interaction between the donor SUVs and the acceptor I-FABP (10), indicating a collision-based mechanism for AOFA transfer from SUVs to I-FABP.

Effect of acceptor I-FABP concentration. The marked increase in AOFA transfer rate from cardiolipin-containing donor SUVs to I-FABP (Fig. 4) was further analyzed. In preliminary studies SUVs containing 25% cardiolipin, 10% NBD-PC, and 65% POPC were used, but these SUVs appeared somewhat unstable, as judged by wide variability in transfer rates at temperatures above 30°C (data not shown). Separate studies showed that the presence of 10% egg PE helped stabilize these anionic vesicles (F. Herr & J. Storch, personal communication), and the AOFA transfer

rates from POPC vesicles to I-FABP in the presence or absence of egg PE were very similar (Fig. 1, panel B). All further experiments were therefore performed with SUVs containing 10% egg PE in addition to 25% cardiolipin and POPC.

Transfer of 12-AS from these SUVs was examined as a function of increasing acceptor I-FABP concentration. As above (Fig. 4), the transfer rate was markedly faster when using SUVs containing 25% cardiolipin (**Fig. 5**). Similar to results obtained for AOFA transfer from POPC vesicles to I-FABP (Fig. 1, panel B), however, we did not observe a proportional increase in transfer rate with increasing concentrations of I-FABP (Fig. 5). Nevertheless, the dramatic increase in transfer rate provides further evidence for a collisional mechanism of AOFA transfer from cardiolipin-containing SUVs to I-FABP. Importantly, this effect cannot be due solely to increased AOFA off-rate from the anionic SUVs, as the magnitude of these effects is comparatively small, as observed with AOFA transfer from cardiolipin-containing SUVs to L-FABP (Fig. 4) or to POPC vesicles (Fig. 2, panel B).

Effect of ionic strength. Increasing ionic strength caused a logarithmic decrease in AOFA transfer rate from cardiolipin-containing SUVs, and at 500 mm NaCl the rate observed with 25% cardiolipin vesicles was equivalent to that obtained with POPC vesicles (**Fig. 6**). As AOFA transfer from cardiolipin vesicles to I-FABP is proposed to not take place by a diffusion-mediated process, as demonstrated by comparison to vesicle-to-vesicle transfer (Fig. 2, panel B), it is suggested that the increased ionic strength probably masks electrostatic interactions between I-FABP and cardiolipin.

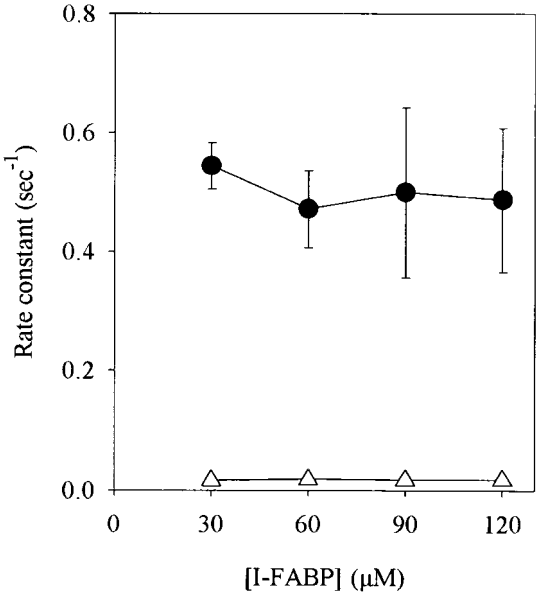

Fig. 5. Effect of 25% cardiolipin-containing vesicles on the rate of AOFA transfer to I-FABP. Transfer of 1 μm 12-AS from 25% cardiolipin-containing vesicles was measured as a function of I-FABP concentration. Data shown for transfer with 25 μm vesicles containing 80%POPC/10% egg PE/10%NBD-PC vesicles (●) or 25% cardiolipin/55% POPC/10% egg PE/10% NBD-PC (●). Data shown for at least three different experiments ± standard deviation.

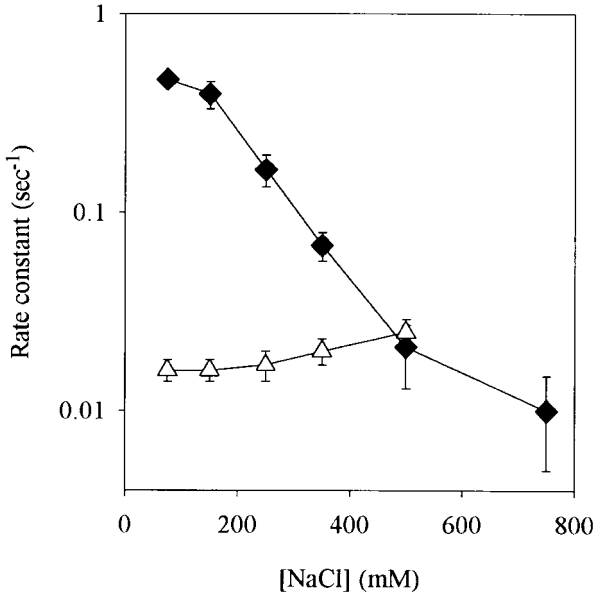

Fig. 6. Ionic strength effect on the AOFA transfer rate from 25% cardiolipin-containing vesicles to I-FABP. Transfer of 1 μm 12-AS from 25 μm vesicles containing 80% POPC/10% egg PE/10% NBD-PC vesicles (△) or 25% cardiolipin/55% POPC/10% egg PE/10% NBD-PC (◆) to I-FABP (30 μm) was measured as a function of NaCl concentration. Data shown for at least three different experiments ± standard deviation.

Effect of temperature. The thermodynamic parameters of AOFA transfer from I-FABP to cardiolipin-containing vesicles were determined by measuring the transfer rate in the temperature range of 5°C–30°C (Table 2). The enthalpic contribution for AOFA transfer from cardiolipin-containing SUVs to I-FABP was higher than for transfer from vesicles containing only POPC and NBD-PC. Further, as described above for POPC vesicles, the major component of $\Delta G^{\ddagger}$ for AOFA transfer from cardiolipin-containing SUVs to I-FABP was enthalpic, with considerably smaller $T\Delta S^{\ddagger}$ contributions relative to transfer from POPC SUVs to L-FABP. Indeed, the small decrease in entropy observed for transfer from POPC to I-FABP was still further diminished when the donor SUVs contained cardiolipin (Table 2). These observations provide further indirect evidence for the absence of a bulk aqueous-phase transfer process and imply that I-FABP and/or vesicle conformational changes may occur during transient interactions between I-FABP and vesicles.

Inter-membrane AOFA transfer. The dramatic increase in AOFA transfer rate from cardiolipin-containing SUVs relative to POPC SUVs (Figs. 4–6) supports the collision-mediated transfer of fatty acid from membranes to I-FABP. Nevertheless, as relatively modest increases in the inter-membrane diffusional transfer rate (approximately 1.5-fold) from negatively charged POPG and PA vesicles were found in earlier studies (27), we could not at this point exclude a direct effect of cardiolipin on the AOFA dissociation rate. Therefore we compared AOFA transfer from POPC or cardiolipin-containing donor vesicles to acceptor POPC vesicles versus L-FABP or I-FABP as acceptor (Fig.

2). This allowed us to determine whether the effects observed with cardiolipin-containing donor vesicles were specific to I-FABP as acceptor (Fig. 4), or whether a similarly large enhancement of AOFA transfer rate from these donors to POPC acceptors would occur. The vesicle-to-vesicle transfer of AOFA is diffusional (19, 27) and the rate of 12-AO transfer from donor POPC or cardiolipin-containing vesicles was similar for either L-FABP or POPC vesicles as the acceptor (Fig. 2, panel A), further suggesting that transfer to L-FABP is also diffusional. The transfer rate from donor cardiolipin-containing vesicles was approximately 2-fold higher than from POPC vesicles (Fig. 2, panel A), an effect which is easily explained by charge–charge repulsion between the negatively charged AOFA and cardiolipin, and is consistent with the effect observed previously for transfer from anionic vesicles (19, 27). In distinct contrast, when transfer to I-FABP was compared to POPC vesicles as acceptor (Fig. 2, panel B) the rate of 12-AS transfer was about 3-fold faster from POPC SUVs and approximately 47-fold faster from cardiolipin-containing SUVs for I-FABP as acceptor. As these transfer rates are markedly different from those obtained for vesicle-to-vesicle transfer (Fig. 2, panel B) it is clear that a protein-specific effect is being observed for transfer to I-FABP which cannot be explained by anomalous behavior of either the vesicles and/or AOFA interactions with phospholipids. The data, therefore, strongly support the hypothesis that AOFA transfer from both neutral and anionic donor SUVs to I-FABP occurs by a process that involves protein–membrane collisional interactions.

DISCUSSION

The suggestion that the FABPs participate in the intracellular transport of long-chain fatty acids (1, 2, 4–6) implies that these proteins may be involved not only in the delivery of ligand to acceptor sites, but also in the extraction of fatty acids from donor sites, for instance their removal from the plasma membrane after trans-membrane transport. In this study we have investigated the mechanism of AOFA transfer from phospholipid membranes to L-FABP or I-FABP and the data suggest that AOFA transfer from membrane vesicles to L-FABP occurs by a diffusion-mediated mechanism, whereas AOFA transfer to I-FABP takes place through a transient collisional interaction. We have previously found that AOFA transfer from L-FABP to membrane vesicles also occurs by a diffusion-mediated process (10, 25, 32). Thus, L-FABP may act as an intra-cellular reservoir for fatty acids, with ligand dissociation into the aqueous phase regulating rates of transfer between membranes and protein. For movement of fatty acids between membranes and I-FABP, on the other hand, a collision-mediated mechanism is hypothesized for transfer from membranes to proteins, and a comparable transfer mechanism was also demonstrated for transfer from I-FABP to membranes (10). However, the putative I-FABP-membrane collisional complexes that are envisioned to occur in fatty acid transfer in either direction may have different properties, as they would involve membrane contacts with holo-I-FABP versus apo-I-FABP. That such differences may exist is supported, albeit indirectly, by differential kinetic regulation of AOFA transfer between I-FABP and membranes, when transfer in both directions is compared.

In contrast to the proportional increase in AOFA transfer rate with increasing acceptor SUV concentration (Fig. 1, panel D), AOFA transfer from SUVs to I-FABP is not proportional to the concentration of the acceptor I-FABP (Fig. 1, panel B). The observation that transfer rates do not increase with acceptor I-FABP level suggests that the formation of transient collisional complexes between I-FABP and membranes may not be the rate-limiting step in the process of AOFA transfer (35). Rather, it is hypothesized that a conformational change in I-FABP and/or ligand binding to I-FABP occurs more slowly than the I-FABP–membrane interaction, and is consequently rate-limiting for AOFA transfer from membranes to I-FABP. These processes may occur at different rates depending upon the nature of the I-FABP–membrane complex that is formed, and are thereby modulated by membrane type, but not membrane concentration. Thus, formation of the I-FABP–membrane complex does not decrease the AOFA-NBD energy transfer efficiency, but AOFA movement from its membrane site to I-FABP will decrease energy transfer and hence increase AOFA fluorescence intensity. A dependence of the AOFA transfer rate on the binding process, which is secondary to the initial I-FABP–membrane collisional interaction, could explain the absence of an increase in transfer rate with increased acceptor I-FABP concentration, as would otherwise be expected for a collisional transfer process (35, 36).

For AOFA transfer from membranes to I-FABP, we hypothesize that apo-I-FABP interacts with the phospholipid membrane surface, causing a conformational change in I-FABP which thereby facilitates ligand binding. Indeed, structural analysis of the apo- and holo-I-FABP tertiary structures by multidimensional NMR spectroscopy revealed a high degree of flexibility and disorder in discrete regions of apo-I-FABP relative to the holo protein (37, 38). In particular, portions of the α-helical portal domain of I-FABP, specifically the distal half of the α-II helix and the turn between β-strands C and D, were shown to be ordered in the presence of bound fatty acid and disordered in their absence (37, 38). The importance of the I-FABP α-helical domain in collisional fatty acid transfer from protein to membrane acceptors, moreover, was recently demonstrated using a helix-less variant of I-FABP (11). Thus, we suggest that differences in the apo- and holo-I-FABP structures, particularly in the helical region, are probably reflected by subtle differences in the regulation of AOFA transfer from donor I-FABP (10) compared with I-FABP as AOFA acceptor, as demonstrated in this study.

Theoretical analyses of cellular long-chain fatty acid diffusion in the absence or presence of FABPs have demonstrated that these proteins can increase the diffusional flux of ligand under certain conditions (8, 39). One requirement is that there is more protein-bound than unbound ligand, and in this respect intracellular FABP con-

centrations have been estimated at 150 μm–300 μm, with intracellular unbound long-chain fatty acid concentrations maintained at approximately 7 nm by heart FABP, L-FABP, and I-FABP (40–42). Additionally, for FABPs to play a key role in intracellular fatty acid transport, the spontaneous release of fatty acids from membranes must be slow and fatty acids must be taken up directly from membranes by FABP without an aqueous-phase intermediate (8). Similarly, the fatty acids must be delivered directly to membranes via protein–membrane interactions, rather than by dissociation and aqueous-phase diffusion to acceptor membrane sites (8, 9). The present studies demonstrate that I-FABP, but not L-FABP, can "extract" the fatty acid analogue AOFA directly from model membrane vesicles. In addition, our previous studies demonstrated that I-FABP delivers AOFA to membranes via direct collisional interactions (10). Therefore we provide experimental evidence supporting the concept that I-FABP can increase the cytosolic diffusional flux of long-chain fatty acids by transporting these ligands between membranes.

These results indicate that the two FABPs present in intestinal enterocytes, L-FABP and I-FABP, may have different functions in fatty acid transport and utilization (10). It is suggested that I-FABP specifically transfers long-chain fatty acids between membranes to, and from, sites of fatty acid metabolism. On the other hand, L-FABP may have a protective role in buffering the adverse effects of high membrane- or non-protein-bound fatty acid concentrations (10, 25, 32). In addition, for L-FABP, any interactions with biological membranes, as have been reported (43, 44), may not involve L-FABP interactions with membrane lipids, but rather protein–protein interactions, whereas for I-FABP both protein–lipid and protein–protein interactions are possible.

This work was funded by PHS grant DK 38389. We thank Dr. Alan Kleinfeld for supplying the plasmids used to obtain I-FABP and L-FABP.

Manuscript received 17 August 1999 and in revised form 17 December 1999.

REFERENCES

1. Bass, N. M. 1985. Function and regulation of hepatic and intestinal fatty acid binding proteins. *Chem. Phys. Lipids.* **38:** 95–114.
2. Glatz, J. F. C., and G. J. van der Vusse. 1996. Cellular fatty acid-binding proteins—their function and physiological significance. *Prog. Lipid Res.* **35:** 243–282.
3. Storch, J., and A. E. A. Thumser. 2000. The fatty acid transport function of fatty acid binding proteins. *Biochim. Biophys. Acta.* (In press)
4. Storch, J., F. M. Herr, K. T. Hsu, H. K. Kim, H. L. Liou, and E. R. Smith. 1996. The role of membranes and intracellular binding proteins in cytoplasmic transport of hydrophobic molecules: fatty acid-binding proteins. *Comp. Biochem. Physiol.* **115:** 333–339.
5. Veerkamp, J. H., and R. G. H. J. Maatman. 1995. Cytoplasmic fatty acid-binding proteins: their structure and genes. *Prog. Lipid Res.* **34:** 17–52.
6. Banaszak, L. J., N. Winter, Z. Xu, D. A. Bernlohr, and T. A. Jones. 1994. Lipid-binding proteins: a family of fatty acid and retinoid transport proteins. *Adv. Prot. Chem.* **145:** 90–148.
7. Sacchettini, J. C., and J. I. Gordon. 1993. Rat intestinal fatty acid binding protein. A model system for analyzing the forces that can bind fatty acids to proteins. *J. Biol. Chem.* **268:** 18399–18402.
8. Vork, M. M., J. F. C. Glatz, and G. J. van der Vusse. 1997. Modeling intracellular fatty acid transport—possible mechanistic role of cytoplasmic fatty acid-binding protein. *Prostaglandins Leukotrienes Essent. Fatty Acids.* **57:** 11–16.
9. Vork, M. M., J. F. Glatz, and G. J. van der Vusse. 1993. On the mechanism of long chain fatty acid transport in cardiomyocytes as facilitated by cytoplasmic fatty acid-binding protein. *J. Theor. Biol.* **160:** 207–222.
10. Hsu, K. T., and J. Storch. 1996. Fatty acid transfer from liver and intestinal fatty acid-binding proteins to membranes occurs by different mechanisms. *J. Biol. Chem.* **271:** 13317–13323.
11. Corsico, B., D. P. Cistola, C. Frieden, and J. Storch. 1998. The helical domain of intestinal fatty acid binding protein is critical for collisional transfer of fatty acids to phospholipid membranes. *Proc. Natl. Acad. Sci. USA.* **95:** 12174–12178.
12. Richieri, G. V., R. T. Ogata, and A. M. Kleinfeld. 1992. A fluorescently labeled intestinal fatty acid binding protein. Interactions with fatty acids and its use in monitoring free fatty acids. *J. Biol. Chem.* **267:** 23495–23501.
13. Maniatis, T., E. F. Fritsch, and J. F. Sambrook. 1982. Molecular Cloning: A Laboratory Manual. Cold Spring Harbor Laboratory, Cold Spring Harbor, New York.
14. Kim, H. K., and J. Storch. 1992. Mechanism of free fatty acid transfer from rat heart fatty acid-binding protein to phospholipid membranes. Evidence for a collisional process. *J. Biol. Chem.* **267:** 20051–20056.
15. Glatz, J. F. C., and J. H. Veerkamp. 1983. A radiochemical procedure for the assay of fatty acid binding by proteins. *Anal. Biochem.* **132:** 89–95.
16. Laemmli, U. K. 1970. Cleavage of structural proteins during the assembly of the head of bacteriophage T_4. *Nature.* **227:** 680–685.
17. Bradford, M. 1976. A rapid and sensitive method for the quantitation of microgram quantities of protein utilizing the principle of protein-dye binding. *Anal. Biochem.* **72:** 248–254.
18. Hubbell, T., W. D. Behnke, J. K. Woodford, and F. Schroeder. 1994. Recombinant liver fatty acid binding protein interacts with fatty acyl-coenzyme. *Biochemistry.* **33:** 3327–3334.
19. Storch, J., and A. M. Kleinfeld. 1986. Transfer of long-chain fluorescent free fatty acids between unilamellar vesicles. *Biochemistry* **25:** 1717–1726.
20. Huang, C., and T. E. Thompson. 1974. Preparation of homogeneous, single-walled phosphatidylcholine vesicles. *Methods Enzymol.* **32:** 485–489.
21. Gomori, G. 1942. A modification of the colorimetric phosphorous determination for use with the photoelectric colorimeter. *J. Lab. Clin. Med.* **27:** 955–960.
22. Massey, J. B., D. H. Bick, and H. J. Pownall. 1997. Spontaneous transfer of monoacyl amphiphiles between lipid and protein surfaces. *Biophys. J.* **72:** 1732–1743.
23. Storch, J. 1990. Mechanism for binding of fatty acids to hepatocyte plasma membranes - different interpretation. *Hepatology.* **12:** 1447–1449.
24. Roseman, M. A., and T. E. Thompson. 1980. Mechanism of the spontaneous transfer of phospholipids between bilayers. *Biochemistry.* **19:** 439–444.
25. Storch, J., and N. M. Bass. 1990. Transfer of fluorescent fatty acids from liver and heart fatty acid-binding proteins to model membranes. *J. Biol. Chem.* **265:** 7827–7831.
26. Wootan, M. G., and J. Storch. 1994. Regulation of fluorescent fatty acid transfer from adipocyte and heart fatty acid binding proteins by acceptor membrane lipid composition and structure. *J. Biol. Chem.* **269:** 10517–10523.
27. Sunderland, J. E., and J. Storch. 1993. Effect of phospholipid headgroup composition on the transfer of fluorescent long-chain free fatty acids between membranes. *Biochim. Biophys. Acta.* **1168:** 307–314.
28. Glasstone, S., K. Laidler, and E. Eyring. 1941. The Theory of Rate Processes. McGraw-Hill, New York. 100
29. Storch, J. 1990. A comparison of heart and liver fatty acid-binding proteins: interactions with fatty acids and possible functional differences studied with fluorescent fatty acid analogues. *Mol. Cell. Biochem.* **98:** 141–147.
30. Tanford, C. 1980. The Hydrophobic Effect: Formation of Micelles and Biological Membranes. Wiley-Interscience, New York.
31. Charlton, S. C., and L. C. Smith. 1982. Kinetics of transfer of pyrene and rac-1-oleyl-2-[4-(3-pyrenyl)butanoyl]glycerol between human plasma lipoproteins. *Biochemistry.* **21:** 4023–4030.
32. Kim, H. K., and J. Storch. 1992. Free fatty acid transfer from rat

liver fatty acid-binding protein to phospholipid vesicles. Effect of ligand and solution properties. *J. Biol. Chem.* **267:** 77–82.
33. Herr, F. M., J. Aronson, and J. Storch. 1996. Role of portal region lysine residues in electrostatic interactions between heart fatty acid binding protein and phospholipid membranes. *Biochemistry.* **35:** 1296–1303.
34. Shinitzky, M., and P. Henkart. 1979. Fluidity of cell membranes - current concepts and trends. *Int. Rev. Cytol.* **60:** 121–147.
35. Duckwitz-Peterlein, G., and H. Moraal. 1978. Transport of lipids through water as exchange mechanism between two liposome populations. *Biophys. Struct. Mech.* **4:** 315–326.
36. Thilo, L. 1977. Kinetics of phospholipid exchange between bilayer membranes. *Biochim. Biophys. Acta.* **469:** 326–334.
37. Hodsdon, M. E., and D. P. Cistola. 1997. Discrete backbone disorder in the nuclear magnetic resonance structure of apo intestinal fatty acid-binding protein: implications for the mechanism of ligand entry. *Biochemistry.* **36:** 1450–1460.
38. Hodsdon, M. E., and D. P. Cistola. 1997. Ligand binding alters the backbone mobility of intestinal fatty acid-binding protein as monitored by N-15 NMR relaxation and H-1 exchange. *Biochemistry.* **36:** 2278–2290.
39. Tipping, E., and B. Ketterer. 1981. The influence of soluble binding proteins on lipophile transport and metabolism in hepatocytes. *Biochem. J.* **195:** 441–452.
40. Richieri, G. V., R. T. Ogata, and A. M. Kleinfeld. 1994. Equilibrium constants for the binding of fatty acids with fatty acid binding proteins from adipocyte, intestine, heart, and liver measured with the fluorescent probe ADIFAB. *J. Biol. Chem.* **269:** 23918–23930.
41. Richieri, G. V., A. Anel, and A. M. Kleinfeld. 1993. Interactions of long-chain fatty acids and albumin: Determination of free fatty acid levels using the fluorescent probe ADIFAB. *Biochemistry.* **32:** 7574–7580.
42. Bass, N. M., R. M. Kaikaus, and R. K. Ockner. 1993. Physiology and molecular biology of hepatic cytosolic fatty acid-binding protein. *In* Hepatic Transport and Bile Secretion. Physiology and Pathophysiology. N. Tavaloni and P. D. Berk, editors. Raven Press, New York. 421–446.
43. Bordewick, U., M. Heese, T. Borchers, H. Robeneck, F. Spener, and H. Robenek. 1989. Compartmentation of hepatic fatty-acid-binding protein in liver cells and its effect on microsomal phosphatidic acid biosynthesis. *Biol. Chem. Hoppe-Seyler.* **370:** 229–238.
44. Spener, F., C. Unterberg, T. Borchers, and R. Grosse. 1990. Characteristics of fatty acid-binding proteins and their relation to mammary-derived growth inhibitor. *Mol. Cell. Biochem.* **98:** 57–68.